Biophysical Chemistry 187–188 (2014) 1–6

Contents lists available at ScienceDirect

Biophysical Chemistry

journal homepage: http://www.elsevier.com/locate/biophyschem

Bilayer surface association of the pHLIP peptide promotes extensive backbone desolvation and helically-constrained structures

Mia C. Brown, Rauta A. Yakubu, Jay Taylor, Christopher M. Halsey, Jian Xiong, Renee D. JiJi, Jason W. Cooley *

Department of Chemistry, University of Missouri, Columbia, MO 65211, United States

HIGHLIGHTS

- Membrane-associated pHLIP has the same solvation state as membrane-inserted pHLIP.
- Membrane-associated pHLIP has a significant portion of helical structure.
- The amide I is more strongly correlated with backbone solvation than structure.

GRAPHICAL ABSTRACT

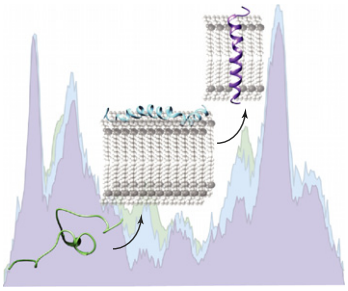

ARTICLE INFO

Article history:
Received 10 September 2013
Received in revised form 15 November 2013
Accepted 15 December 2013
Available online 28 December 2013

Keywords:
Deep-UV resonance Raman spectroscopy
pHLIP
Amide I
Structural transition
Membrane protein

ABSTRACT

Despite their presence in many aspects of biology, the study of membrane proteins lags behind that of their soluble counterparts. Improving structural analysis of membrane proteins is essential. Deep-UV resonance Raman (DUVRR) spectroscopy is an emerging technique in this area and has demonstrated sensitivity to subtle structural transitions and changes in protein environment. The pH low insertion peptide (pHLIP) has three distinct structural states: disordered in an aqueous environment, partially folded and associated with a lipid membrane, and inserted into a lipid bilayer as a transmembrane helix. While the soluble and membrane-inserted forms are well characterized, the partially folded membrane-associated state has not yet been clearly described. The amide I mode, known to be sensitive to protein environment, is the same in spectra of membrane-associated and membrane-inserted pHLIP, indicating comparable levels of backbone dehydration. The amide S mode, sensitive to helical structure, indicates less helical character in the membrane-associated form compared to the membrane-inserted state, consistent with previous findings. However, the structurally sensitive amide III region is very similar in both membrane-associated and membrane-inserted pHLIP, suggesting that the membrane-associated form has a large amount of ordered structure. Where before the membrane-associated state was thought to contain mostly unordered structure and reside in a predominantly aqueous environment, we have shown that it contains a significant amount of ordered structure and rests deeper within the lipid membrane.

1. Introduction

Membrane proteins carry out numerous tasks of wide ranging importance to any membrane-enclosed compartment (from organisms to organelles). They perform essential functions in nearly every aspect of modern biology, medicine, agriculture, and pharmacy [1–5], yet

* Corresponding author at: Department of Chemistry, University of Missouri, 125 Chemistry Bldg., Columbia, MO 65211, United States. Tel.: +1 573 884 7525; fax: +1 573 882 2754.
E-mail address: cooleyjw@missouri.edu (J.W. Cooley).

0301-4622/$ – see front matter © 2013 Elsevier B.V. All rights reserved.
http://dx.doi.org/10.1016/j.bpc.2013.12.004

they are the least understood at the structural and functional levels of all proteins [6]. Most protein dynamics analyses of soluble proteins are carried out by either advanced 2D-NMR methodologies, which are limited to smaller protein molecules and those with relatively slow motions, or by vibrational spectroscopies, including both IR and Raman methodologies. Vibrational spectroscopic techniques are extremely sensitive to changes in the ensemble secondary structure, but are generally not limited by macromolecular size or solvent polarity, unlike modern NMR methodologies. Thus, vibrational methodologies have been at the forefront of studies of conformational changes in peptides and proteins [7–13].

The peptide bond of a protein backbone gives rise to four principle vibrational modes, termed the amide I, II, III and S ($C_\alpha - H$ bending) bands. The position and intensity of these bands are dependent upon the protein's secondary structure [14–16]. Therefore, the observed IR and Raman bands (all four modes) are the sum of the contributions from each peptide bond as a function of the constraints applied by the secondary structure within which they are found. The amide modes are resonantly enhanced in Raman spectra when deep-UV radiation ($\lambda_{ex} < 210$ nm) is used as the excitation source, making deep-UV resonance Raman (dUVRR) an excellent method for studying protein structure [17–19] and dynamics [9,20–26].

The common secondary structures of soluble proteins, α-helix, β-sheet, and disordered, each gives rise to discrete dUVRR spectral profiles, the intensity of which is determined by the relative amount of each structure, making the total spectrum a sum of the underlying structural content [27]. The resolving power of dUVRR to deconvolute this secondary structure content has been demonstrated several fold [25,27–31].

The increased sensitivity of dUVRR over analogous techniques, such as circular dichroism (CD) has demonstrated that the structure of disordered proteins is not random, but a mixture of extended helical (PPII) [32–34] and β-strand structures [35,36]. Recently, it was shown that at an excitation wavelength of 197.5 nm, the turn content could be resolved from the unfolded structure [28]. CD is also capable of resolving unfolded or intermediate structures from one another by the presence of a small positive feature at 220 nm that is distinctly characteristic of PPII structure [36]. However, this feature is not resolved in the presence of any helical or sheet structure. Alternatively, PPII and β-strand structures can readily be distinguished from one another using dUVRR spectroscopy regardless of the nature of the secondary structural content by using the position of the amide III band [35]. In addition to structural information, it has also been shown that dUVRR is sensitive to the environment of the peptide backbone. The amide I mode of dUVRR spectra has been shown to be sensitive to lipid solvation of the peptide backbone [37]. This allows for the observation of both structural and environmental changes of peptides and proteins.

Here we extend these previous studies to a peptide that has the ability to simultaneously undergo both structural and environmental transitions. The pH low insertion peptide (pHLIP), derived from the *c*-helix of the transmembrane protein, bacteriorhodopsin [38], is an ideal model for the analysis of such a system. It undergoes a variety of structural changes dependent on pH and the presence of a lipid bilayer. In the absence of a lipid environment, at low concentration (~10 μM), the peptide is monomeric and mostly disordered [38–40]. At high pH in the presence of liposomes, the peptide associates with the lipid bilayer and loses a portion of its disordered content. Finally, as the pH drops below 6.0 in the presence of lipid, pHLIP spontaneously inserts into the lipid bilayer as a transmembrane α-helix [38–42]. While it has been determined that these three distinct states exist, the exact nature of the membrane–lipid interactions and structural composition of each state have not been fully elucidated.

It has been demonstrated that dUVRR has the ability to resolve discrete and subtle contributions of secondary structure, without the use of spin labels, expensive isotope labeling, or deuterium exchange. Analysis of protein structural changes within native lipid environments without the need for modification would lead to significant improvements in our understanding of membrane proteins, which are widely involved in sensing, transporting, and signaling across lipid barriers.

2. Materials and methods

2.1. Lipid vesicle preparation

DMPC (1,2-dimyristoyl(d54)-*sn*-glycero-3-phosphocholine) (Avanti Polar Lipids) powder was dissolved in chloroform and 12.5 mg quantities were aliquoted into glass test tubes, dried under an argon stream, and placed under vacuum overnight. Lipids were rehydrated in buffer (10 mM phosphate, pH 7.4) and sonicated at 58 °C for 1 h. Lipid solutions were then extruded through a 100 nm pore sized membrane to produce small unilamellar vesicles. Vesicle size distribution was verified via dynamic light scattering (DLS) on a DynaPro99 (Protein Solutions, Charlottesville, VA). Lipid concentration was determined using the Rouser phosphorous assay [43].

2.2. Sample preparation for DUVRR

The pHLIP (Pi Proteomics) peptide was resuspended in hexafluoroisopropanol (HFIP) at 6.25 mg/mL and aliquoted into glass tubes in 62.5 μg quantities. Tubes were dried under an argon stream and placed under vacuum overnight to remove any residual solvent. DMPC vesicles were added to each tube of pHLIP such that the ratio of peptide:lipid was 1:25. The lipid–pHLIP solution was diluted to 5 mL to prevent peptide aggregation. Solutions from each tube were combined and brought to pH 4 with phosphoric acid, resulting in peptide insertion into the membrane. The solution was then centrifuged at 45,000 r.p.m. for 1 h to pellet the proteoliposomes. The pellet was then resuspended in 100 mM phosphate buffer at pH 4 with 100 mM $NaClO_4$. The solution was then split into two equal volumes, one of which was adjusted to pH 7 using NaOH to promote pHLIP association with the membrane surface, and one which was kept at pH 4 to maintain pHLIP as a transmembrane helix.

2.3. Circular dichroism (CD)

CD spectra were collected on a Jasco J-815 CD spectropolarimeter (Easton, MD) using a Hellma cuvette with a pathlength of 10 mm. Five scans were collected and averaged for each sample. As CD measurements do not require a high protein concentration, the protein concentrations were 0.0125 mg/mL in a buffer of 100 mM phosphate and 100 mM $NaClO_4$ at pH 4 or 7. For spectra of membrane-associated and inserted states, lipid was added to a final concentration of 0.3125 mg/mL.

2.4. Deep UV resonance Raman (dUVRR)

The dUVRR instrument was set up as described previously [44]. Briefly, the fourth harmonic of a tunable titanium–sapphire laser at excitation wavelengths of 195, 197, 199, 201, 203, or 205 nm was directed onto a thin film of sample flowing between two nitinol wires spaced approximately 1 mm apart under N_2 gas. The incident laser power at the sample was attenuated to 500 μW to avoid protein degradation, and spectra were monitored for degradation over time using the aromatic ring modes. Spectral calibration was carried out using a standard cyclohexane spectrum [45]. All dUVRR spectral preprocessing was carried out in MATLAB (7.1, MathWorks, Natick, MA) using cosmic ray and water band removal methods described previously [31]. A nonlinear least-squares algorithm was used to fit the amide and aromatic bands to mixed Gaussian/Lorentzian peaks, which approximate the Voigt line shape as described previously [30].

3. Results

3.1. CD spectra

Previous studies of pHLIP have shown that pHLIP adopts three distinct structures depending on its environment [39,40,46]. Circular dichroism (CD) spectroscopy was employed to confirm the presence of a distinct state in each environment. The spectrum of pHLIP in aqueous solution at pH 7 has a single minimum at 201 nm, indicating that the peptide is in a predominantly disordered state (Fig. 1). Upon introduction of DMPC liposomes, the minimum at 201 nm shifts towards 206 nm and decreases in intensity. Additionally, a negative feature begins to appear at 220 nm, suggesting the formation of some α-helical structure. The appearance of α-helical structure upon association with the DMPC membrane surface is consistent with the findings of Engelman and coworkers [38,40]. Upon lowering the pH to 4 the CD spectrum takes on a classically α-helical shape, with two prominent minima at 209 and 222 nm (Fig. 1).

3.2. DUVRR spectra of pHLIP as a function of environment

Although it is clear that pHILP is disordered in an aqueous environment and α-helical when inserted into the membrane at pH 4, the structure of the peptide and nature of the interaction with the membrane at pH 7 remain unclear. In order to elucidate the structure of the membrane-associated peptide at pH 7, dUVRR spectra of pHLIP were measured in each state. The peptide contains two tyrosines, giving rise to an amide III region dominated by tyrosine features, making structural analysis using the amide III difficult. DUVRR spectra of pHLIP in aqueous solution and associated with the DMPC surface exhibit a prominent amide S feature (assigned to an in-plane N – H/C – H coupled bending [47]) (Fig. 2A), indicative of a large amount of non-helical structure, consistent with CD spectra. However, the amide S of membrane-associated pHLIP is not as intense as that seen in the aqueous sample, suggesting an increase in helical structure. In addition, the membrane-associated spectrum also displays a less intense amide II band (predominantly N – H bending) [48] than the aqueous spectrum, further indicating formation of helical structure in the membrane-associated form of the peptide. Despite the obvious structural changes implied by the amide II and amide S bands, there is no accompanying shift in the position of the amide I band (predominantly C═O stretching) [49,50] at 1671 cm^{-1}. There is, however, a marked increase in the intensity of the amide I when pHLIP associates with a membrane. Although the amide I intensity is not strongly correlated with the backbone dihedral angles [49,50], the intensity does increase concurrently with dehydration of the backbone carbonyl [37]. Therefore, the increased intensity of the amide I feature in the membrane-associated spectrum demonstrates decreased hydration of the peptide backbone in this state. Additionally, there is an overall increase in the intensity of the aromatic modes, also suggesting a transfer to a more hydrophobic environment.

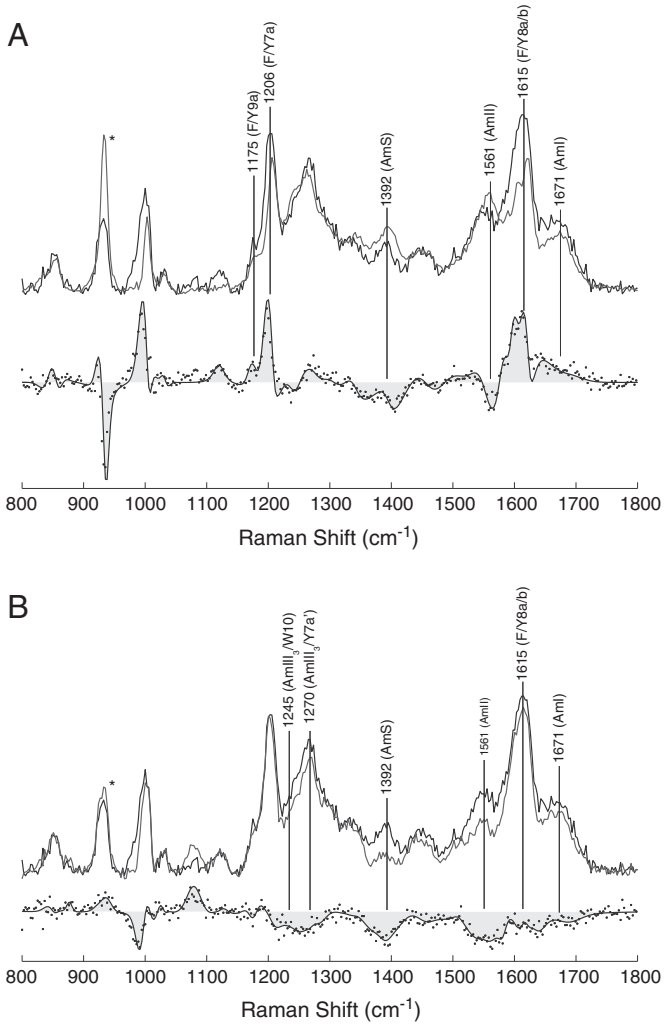

Fig. 2. A. 197 nm-excited DUVRR spectra of pHLIP associated with DMPC at pH 7 (black) and in aqueous buffer at pH 7 (gray) with difference spectrum. B. pHLIP inserted in DMPC at pH 4 (gray) and associated with DMPC at pH 7 (black) with difference spectrum. The peak marked with an asterisk is from the internal standard, NaClO4.

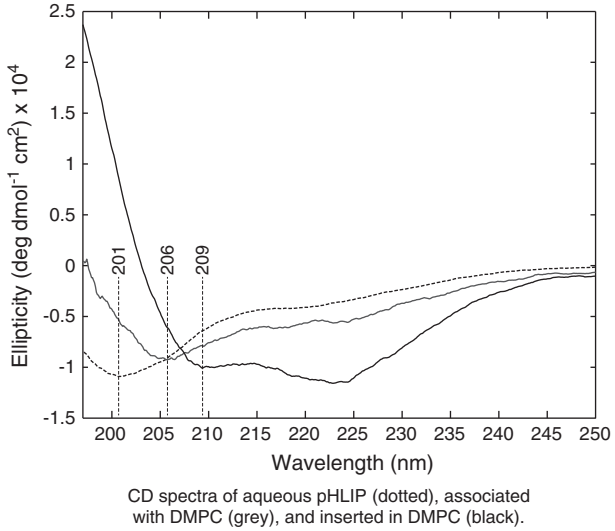

Fig. 1. CD spectra of soluble (dotted), membrane-associated (gray), and membrane-inserted (black) pHLIP.

In contrast to the membrane-associated pHLIP, the spectrum of membrane-inserted pHLIP has a negligible amide S feature and a drastically reduced amide II band (Fig. 2B), which is consistent with previous studies showing that the peptide is significantly moreα-helical when inserted in the membrane [38,40]. There is a negligible change in the intensity of the amide I when pHLIP transitions from a membrane-associated state to the membrane inserted state, implying approximately the same level of backbone dehydration. Once again, there is no accompanying shift in the amide I with the change in structure. These modes are most intense in the membrane-associated state of the peptide and least intense in the aqueous form.

Excitation profiles of the lipid-associated and lipid-inserted forms of pHLIP reveal more subtle spectral differences (Fig. 3). The aromatic

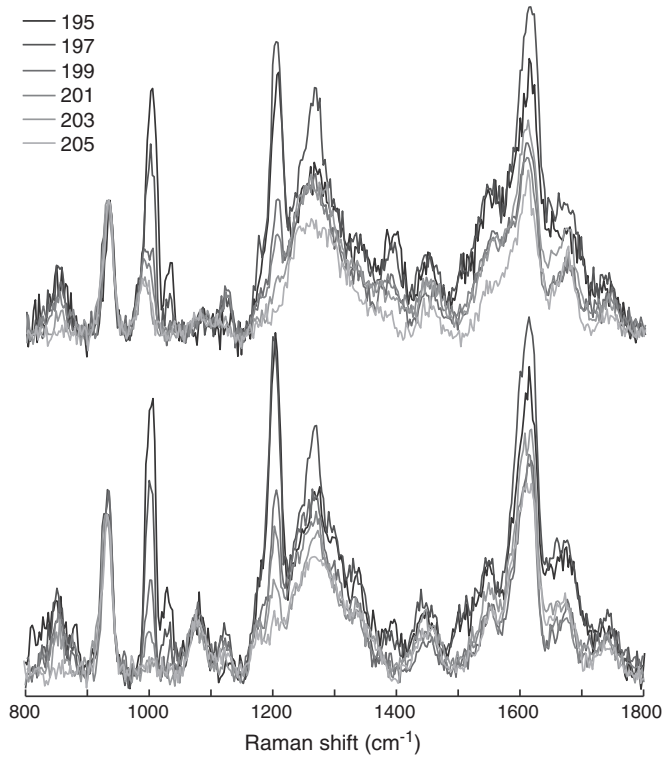

Fig. 3. Excitation profiles of pHLIP associated with DMPC at pH 7 (top) and inserted in DMPC at pH 4 (bottom).

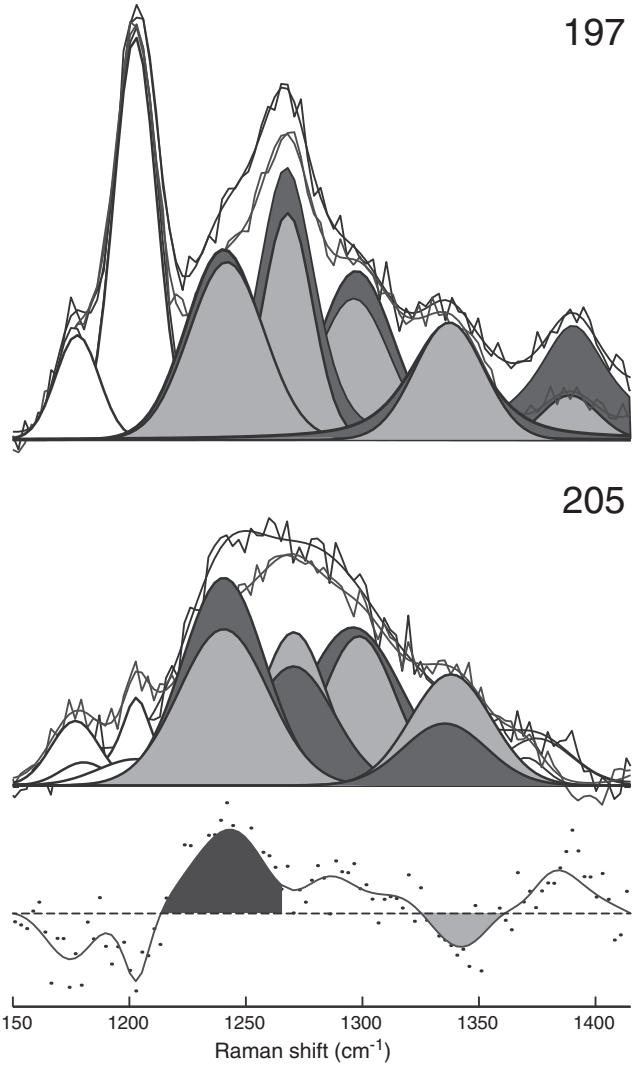

Fig. 4. Spectra of membrane-associated and membrane-inserted pHLIP at 197 nm (top) and 205 nm (middle) excitation, and difference spectrum at 205 nm excitation (bottom). Aromatic modes (white) almost disappear at 205 nm excitation. Amide III modes of membrane-associated pHLIP are represented in dark gray and the membrane inserted in light gray. The amide III_3 component at 1242 cm^{-1} is larger in membrane-associated pHLIP (bottom, dark gray fill), while the helically-associated band at 1338 cm^{-1} is more intense in the membrane-inserted pHLIP (bottom, light gray fill).

modes drop off dramatically with increasing excitation wavelength for both states. In the membrane-inserted state the phenylalanine F12 and F18a modes disappear entirely above 201 nm excitation. In the membrane-associated state the F12 mode remains; however, it decreases in intensity with increasing excitation wavelength. In the membrane-associated spectrum of pHLIP, the region containing the phenylalanine and tyrosine F8a and Y8b modes has a maximum at 1615 cm^{-1} at an excitation wavelength of 195 nm. This maximum shift towards 1611 cm^{-1} as the excitation wavelength is increased. As the Y8b generally has a peak maximum at about 1620 cm^{-1}, and that of the F8a rests at approximately at 1600 cm^{-1}, this indicates that the Y8b mode is decreasing at a faster rate than the F8a mode with increasing wavelength. This trend is not observed in the excitation spectra of membrane-inserted pHLIP. The region containing the phenylalanine and tyrosine 9a and 7a modes at 1178 and 1203 cm^{-1} respectively decreases in intensity in both spectra, but disappears more quickly in the membrane-associated spectrum. As the aromatic modes in this region decrease so drastically with an excitation wavelength above 201 nm, the contribution from tyrosine in the amide III region should be minimal above 201 nm excitation.

Changes in the amide III region are more easily resolved at excitation wavelengths above 201 nm due to the decreased contribution from aromatic modes. Clear differences are seen between the spectra of the membrane-associated and membrane-inserted forms of pHLIP. The amide III region can be resolved into four bands, two bands that make up the amide III_3 [51] (Fig. 4), and two bands generally associated with alpha-helical structure at 1300 and 1330 cm^{-1}. As the excitation wavelength increases, the amide modes generally decrease in intensity in spectra of both forms of pHLIP. In both sets of spectra, the amide S disappears entirely. There is very little change in the amide III region modes at 1270 cm^{-1} in both spectra; however, while there is no change in the mode at 1335 cm^{-1} in the membrane-inserted spectrum, there is a marked decrease in intensity at this position in the membrane-associated spectrum. The band at 1270 cm^{-1} remains in both sets of spectra as the excitation wavelength increases. However, while the band 1245 cm^{-1} remains in the membrane-associated spectrum, it experiences a more drastic decrease in the membrane-inserted spectrum. The comparative increased intensity of the 1245 cm^{-1} band and decreased intensity of the 1335 cm^{-1} band in the membrane-associated spectrum suggest both an increase in disordered structure and a loss in α-helical content. As previously shown by Asher and coworkers, the shift of the amide III_3 band can be used to predict the psi angle to within ±8° using Eq. (1) [52]:

$$\vartheta_{III3}^{EXT} = 1256\mathrm{cm}^{-1} - 54\mathrm{cm}^{-1}\sin(\psi + 26^{\circ}). \quad (1)$$

Using this relationship, the residual intensity at 1242 cm^{-1} in the difference spectra corresponds to extended helical structure.

In addition to a more defined amide III region, excitation spectra also provide more detailed structural information with regard to the amide II region. The amide II band in the membrane-associated spectrum decreases more rapidly than in the membrane-inserted spectrum (Fig. 5). Previous data has shown that the amide II mode of α-helical proteins decreases more slowly with increasing excitation wavelength than that

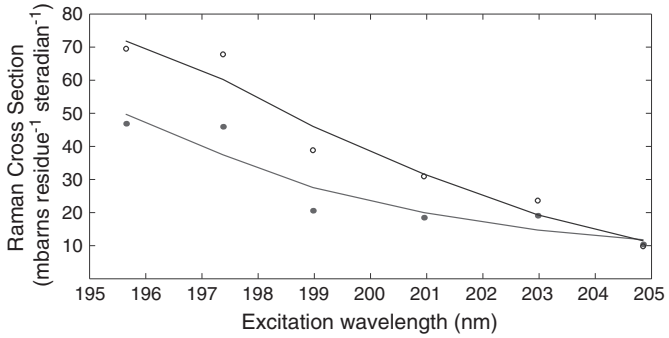

Fig. 5. Raman cross sections of the amide II mode of membrane-associated pHLIP (black) decrease more quickly than membrane-inserted pHLIP (gray). Lines have been included to guide the eye.

of non-helical proteins [30], implying a larger portion of non-helical structure in the membrane-associated form of pHLIP compared to the membrane-inserted form.

4. Discussion

Three structural states of pHLIP, aqueous, membrane-associated, and membrane-inserted have been identified by CD [38–40]. CD studies show that in aqueous solution, pHLIP is mostly disordered and folded in an α-helical conformation when inserted into a membrane. However, our understanding of the structural content of membrane-associated pHLIP remains vague. Molecular dynamics simulations suggest a significant portion of helical character [53]; however, detailed experimental data is sparse. CD spectra of membrane-associated pHLIP display helical characteristics, such as a minimum around 220 nm; however, it is less intense than in spectra of membrane-inserted pHLIP (Fig. 1 and [38–40]). Membrane-inserted pHLIP exhibits a minimum at 210 nm, but the minimum in the membrane-associated form is shifted slightly to 206 nm. These changes indicate a decrease in helical structure, concomitant with an increase in unordered structure. While this presents a vague picture of the structural ensemble of membrane-associated pHLIP, a more exact determination of the amounts of helical and unordered structure has not been conducted.

The dUVRR spectra of soluble and membrane-associated pHLIP both have intense amide S and II modes compared to the membrane-inserted form, consistent with larger portions of non-helical structure (Fig. 2). Excitation spectra of membrane-associated and membrane-inserted pHLIP provide more specific structural and environmental differences between these two states, as contribution from aromatic modes is minimized in the amide III region above 201 nm excitation. At 205 nm excitation, the amide III region shows increased intensity around 1242 cm^{-1} in spectra of membrane-associated pHLIP compared to the membrane-inserted state, which is consistent with more extended helical structure (Fig. 4). Additionally, it can be clearly seen that the α-helical-associated mode at 1338 cm^{-1} is smaller in the spectrum of membrane-associated pHLIP. Together, these suggest an incompletely wound helix in the membrane-associated state that completes the folding process upon insertion into the membrane.

The solvation states of aqueous and membrane-inserted pHLIP have been well characterized [38–40,46]; however, the position within the membrane, as well as a more exact structural description, of the membrane-associated state has yet to be determined. Previous work has shown that for membrane-associated and membrane-inserted pHLIP, two environmental populations of tryptophan are present [39,40]. In the membrane-inserted state, both tryptophan residues are buried at varying depths within the membrane. In the membrane-associated state, one tryptophan residue is mostly solvent exposed, while the other is more buried within the membrane [40]. The partial burial of one tryptophan indicates that some portion of membrane-associated pHLIP is at least partially desolvated when bound to the surface of a vesicle [40]; however, the extent of desolvation of the peptide as a whole is unclear.

DUVRR has been used extensively to characterize soluble proteins, but far fewer studies have applied the technique to the study of membrane proteins. In spectra of soluble proteins, the Raman shifts and intensities of all four amide modes are correlated to various types of secondary structure. Recently, Halsey et al. found that spectra of a detergent solvated α-helical protein exhibit a vastly increased amide I mode intensity compared to a different, but similarly structured soluble protein, demonstrating that the amide I is sensitive to the hydration state of the peptide backbone [37]. More recent work on melittin, the hemolytic component of bee venom, found that upon the transition from an aqueous solution to a lipid environment, the intensity and position of the amide I shifted as a result of the changing structure and solvation environment [54].

Unlike the melittin study, the amide I in the pHLIP spectra does not follow the same trends with changes in structure and solvation state. When pHLIP transitions from the soluble to membrane-associated state, there is no accompanying downward shift in the amide I mode, which would be expected with the formation of helical structure (Fig. 2). However, upon association with the lipid bilayer, there is an increase in the intensity of the amide I, suggesting some degree of desolvation of the peptide backbone. This is also supported by the increased intensity of the aromatic modes upon membrane-association, which are expected to increase upon introduction to a more hydrophobic environment.

Upon transitioning from the membrane-associated to membrane-inserted state there is neither a shift in frequency or change in intensity of the amide I (Fig. 2). The lack of change of amide I intensity when converting from the membrane-associated to the membrane-inserted state indicates that the peptide backbone maintains equivalent levels of dehydration in each of these states. However, there are some differences in the environment of the aromatic residues. Although the aromatic region around 1600 cm^{-1} is similar for both states at each wavelength, the region containing the phenylalanine and tyrosine 7a/9a modes decreases more quickly in the membrane-associated spectra (Fig. 4). Generally, this suggests that the phenylalanine and tyrosine residues are in a slightly more hydrophobic environment in the membrane-inserted state.

Although there are obvious structural changes between each state of pHLIP, the peak maximum of the amide I does not change accordingly, while the intensity does change with desolvation. In studies conducted with melittin, both the intensity and position of the amide I changed [54]. Melittin transitions from a completely disordered state to a completely ordered state; however, each form of pHLIP does have some structural order. The structural changes experienced by melittin upon insertion into a lipid bilayer are more drastic than those experienced by pHLIP as it transitions between states. This suggests that the amide I is more sensitive to changes in the solvation state of the peptide backbone than it is to protein structure changes.

5. Conclusions

Using DUVRR, the membrane-associated state of pHLIP has finally been more fully characterized. Instead of being mostly disordered and exposed to solvent on the surface of a membrane as previously thought, it contains mostly ordered structure, and nestled deeper within the membrane surface, having about the same level of desolvation as the inserted form. Additionally, this represents the first study using DUVRR to track the structural transitions and environmental changes of a peptide from a disordered state in an aqueous environment to a fully ordered state in a lipid environment, presenting DUVRR as a powerful tool in future work with membrane proteins.

Acknowledgments

The authors gratefully acknowledge the support from the National Science Foundation CAREER Award CHE-1151533, National Institute of Health EXPRESS grant, the Research Board grant, and the University of Missouri, Department of Chemistry.

References

[1] A. Badou, M.K. Jha, D. Matza, R.A. Flavell, Emerging roles of L-type voltage-gated and other calcium channels in T lymphocytes, Front. Immunol. 4 (2013).
[2] E.L. Eskelinen, Y. Tanaka, P. Saftig, At the acidic edge: emerging functions for lysosomal membrane proteins, Trends Cell Biol. 13 (2003) 137–145.
[3] J.D. Muller, N. Wu, K. Palczewski, Vertebrate membrane proteins: structure, function, and insights from biophysical approaches, Pharmacol. Rev. 60 (2008) 43–78.
[4] J.N. Sachs, D.M. Engelman, Introduction to the membrane protein reviews: the interplay of structure, dynamics, and environment in membrane protein function, Annu. Rev. Biochem. 75 (2006) 707–712.
[5] S. Urban, S.W. Dickey, The rhomboid protease family: a decade of progress on function and mechanism, Genome Biol. 12 (2011).
[6] S.H. White, Biophysical dissection of membrane proteins, Nature 459 (2009) 344–346.
[7] L.D. Barron, L. Hecht, G. Wilsn, The lubricant of life: a proposal that solvent water promotes extremely fast conformational fluctuations in mobile heteropolypeptide structure, Biochemistry 36 (1997) 13143–13147.
[8] R.H. Callender, R.B. Dyer, R. Gilmanshin, W.H. Woodruff, Fast events in protein folding: the time evolution of primary processes, Annu. Rev. Phys. Chem. 49 (1998) 173–202.
[9] I.K. Lednev, A.S. Karnoup, M.C. Sparrow, S.A. Asher, Nanosecond UV resonance Raman examination of initial steps in alpha-helix secondary structure evolution, J. Am. Chem. Soc. 121 (1999) 4076–4077.
[10] R.B. Dyer, F. Gai, W.H. Woodruff, Infrared studies of fast events in protein folding, Acc. Chem. Res. 31 (1998) 709–716.
[11] C.M. Phillips, Y. Mizutani, R.M. Hochstrasser, Ultrafast thermally-induced unfolding of RNase-A, Proc. Natl. Acad. Sci. U. S. A. 92 (1995) 7292–7296.
[12] C.Y. Huang, Z. Getahun, Y. Zhu, J.W. Klemke, W.F. DeGrado, F. Gai, Helix formation via conformation diffused search, Proc. Natl. Acad. Sci. U. S. A. 99 (2002) 2788–2793.
[13] C.Y. Huang, G. Balakrishnan, T.G. Spiro, Early events in apomyoglobin unfolding probed by laser T-jump/UV resonance Raman spectroscopy, Biochemistry 44 (2005) 15734–15742.
[14] M.C. Chen, R.C. Lord, Laser-excited Raman-spectroscopy of biomolecules. IV. Some polypeptides as conformational models, J. Am. Chem. Soc. 96 (1974) 4750–4752.
[15] P.C. Painter, J.L. Koenig, Solution conformation of poly(L-lysine) — Raman and infrared spectroscopic study, Biopolymers 15 (1976) 229–240.
[16] M. Jackson, P.I. Haris, D. Chapman, Conformational transitions of poly(L-lysine): studies using Fourier transform infrared spectroscopy, Biochim. Biophys. Acta Protein Struct. Mol. Enzymol. 998 (1989) 75–79.
[17] R.A. Copeland, T.G. Spiro, Secondary structure determination in proteins from deep (192–223 nm) ultraviolet resonance Raman-spectroscopy, Biochemistry 26 (1987) 2134–2139.
[18] S.H. Song, S.A. Asher, UV resonance Raman studies of peptide conformation in poly(L-lysine), poly(L-glutamic acid), and model complexes — the basis for protein secondary structure determinations, J. Am. Chem. Soc. 111 (1989) 4295–4305.
[19] V.A. Shashilov, V. Sikirzhytski, L.A. Popova, I.K. Lednev, Quantitative methods for structural characterization of proteins based on deep UV resonance Raman spectroscopy, Methods 52 (2010) 23–37.
[20] S.A. Asher, A.V. Mikhonin, S. Bykov, UV Raman demonstrates that alpha-helical polyalanine peptides melt to polyproline II conformations, J. Am. Chem. Soc. 126 (2004) 8433–88440.
[21] G. Balakrishnan, Y. Hu, G.M. Bender, Z. Getahun, W.F. DeGrado, T.G. Spiro, Enthalpic and entropic stages in α-helical peptide unfolding, from laser T-jump/UV Raman spectroscopy, J. Am. Chem. Soc. 129 (2007) 12801–12808.
[22] G. Balakrishnan, C.L. Weeks, M. Ibrahim, A.V. Soldatova, T.G. Spiro, Proteins dynamics from time resolved UV Raman spectroscopy, Curr. Opin. Struct. Biol. 18 (2008) 623–629.
[23] R.D. JiJi, G. Balakrishnan, Y. Hu, T.G. Spiro, Intermediacy of poly(L-proline) II and β-strand conformations in poly(L-lysine) β-sheet formation, probed by temperature-jump/UV resonance Raman spectroscopy, Biochemistry 45 (2006) 34–41.
[24] I.K. Lednev, A.S. Karnoup, M.C. Sparrow, S.A. Asher, Transient UV Raman spectroscopy finds no crossing barrier between the peptide alpha-helix and fully random coil conformation, J. Am. Chem. Soc. 123 (2001) 2388–2392.
[25] V.A. Shashilov, I.K. Lednev, 2D correlation deep UV resonance Raman spectroscopy of early events of lysozyme fibrillation: kinetic mechanism and potential interpretation pitfalls, J. Am. Chem. Soc. 130 (2008) 309–317.
[26] N.I. Topilina, V.V. Ermolenkov, V. Sikirzhytski, S. Higashiya, I.K. Lednev, J.T. Welch, A de novo designed 11 kDa polypeptide: a model for amyloidogenic intrinsically disordered proteins, Biopolymers 93 (2010) 607–618.
[27] Z. Chi, X.G. Chen, J.S.W. Holtz, S.A. Asher, UV resonance Raman-selective amide vibrational enhancement: quantitative methodology for determining protein secondary structure, Biochemistry 37 (1998) 2854–2864.
[28] C.Y. Huang, G. Balakrishnan, T.G. Spiro, Protein secondary structure from deep-UV resonance Raman spectroscopy, J. Raman Spectrosc. 37 (2006) 277–282.
[29] V.A. Shashilov, M. Xu, V.V. Ermolenkov, I.K. Lednev, Latent variable analysis of Raman spectra for structural characterization of proteins, J. Quant. Spectrosc. Radiat. Transf. 102 (2006) 46–61.
[30] J.V. Simpson, G. Balakrishnan, R.D. JiJi, MCR-ALS analysis of two-way UV resonance Raman spectra to resolve discrete protein secondary structural motifs, Analyst 134 (2009) 138–147.
[31] J.V. Simpson, O. Oshokoya, N. Wagner, J. Liu, R.D. JiJi, Pre-processing of ultraviolet Raman spectra, Analyst 136 (2011) 1239–1247.
[32] A.L. Rucker, T.P. Creamer, Polyproline II helical structure in protein unfolded states: lysine peptides revisited, Protein Sci. 11 (2002) 980–985.
[33] M.L. Tiffany, S. Krimm, New chain conformations of poly(glutamic acid) and polylysine, Biopolymers 6 (1968) 1379–1382.
[34] M.L. Tiffany, S. Krimm, Extended conformations of polypeptides and proteins in urea and guanidine hydrochloride, Biopolymers 12 (1973) 575–587.
[35] A.V. Mikhonin, N.S. Myshakina, S.V. Bykov, S.A. Asher, UV resonance Raman determination of polyproline II, extended 2.51-helix, and β-sheet ψ angle energy landscape in poly-L-lysine and poly-L-glutamic acid, J. Am. Chem. Soc. 127 (2005) 7712–7720.
[36] B.W. Chellgren, T.P. Creamer, Short sequences of non-proline residues can adopt the polyproline II helical conformation, Biochemistry 43 (2004) 5864–5869.
[37] C. Halsey, J. Xiong, O. Oshokoya, J. Johnson, S. Shinde, T.J. Beaty, G. Ghirlanda, R. JiJi, J. Cooley, Simultaneous observation of peptide backbone lipid solvation and α-helical structure by deep-UV resonance Raman spectroscopy, Chembiochem 12 (2011) 2125–2128.
[38] J.F. Hunt, P. Rath, K.J. Rothschild, D.M. Engleman, Spontaneous, pH-dependent membrane insertion of a transbilayer α-helix, Biochemistry 36 (1997) 15177–15192.
[39] Y.K. Reshetnyak, M. Segala, O.A. Andreev, D.M. Engelman, A monomeric membrane peptide that lives in three worlds: in solutions, attached to, and inserted across lipid bilayers, Biophys. J. 93 (2007) 2363–2372.
[40] M. Zoonens, Y.K. Reshetnyak, D.M. Engelman, Bilayer interactions of pHLIP, a peptide that can deliver drugs and target tumors, Biophys. J. 95 (2008) 225–235.
[41] D. Weerakkody, A. Moshnikova, M.S. Thakur, V. Moshnikova, J. Daniels, D.M. Engelman, O.A. Andreev, Y.K. Reshetnyak, Family of pH (low) insertion peptides for tumor targeting, Proc. Natl. Acad. Sci. 110 (2013) 5834–5839.
[42] J. Fendos, F.N. Barrera, D.M. Engelman, Aspartate embedding depth affects pHLIP's insertion pKa, Biochemistry 52 (2013) 4595–4604.
[43] G. Rouser, S. Fleischer, A. Yamamoto, Two dimensional thin-layer chromatographic separation of polar lipids and determination of phospholipids by phosphorous analysis of spots, Lipids 5 (1970) 494–496.
[44] M. Wang, R.D. JiJi, Resolution of localized small molecule — aβ interactions by deep-ultraviolet resonance Raman spectroscopy, Biophys. Chem. 158 (2011) 96–103.
[45] J.R. Ferraro, K. Nakamoto, C.V. Brown, Introductory Raman Spectroscopy, 2nd ed. Academic Press, San Diego, CA, 1994.
[46] J. Tang, F. Gai, Dissecting the membrane binding and insertion kinetics of a pHLIP peptide, Biochemistry 47 (2008) 8250–8252.
[47] Y. Wang, R. Purrello, T. Jordan, T.G. Spiro, UVRR spectroscopy of the peptide bond. 1. Amide S, a nonhelical structure marker, is a C.alpha.H bending mode, J. Am. Chem. Soc. 113 (1991) 6359–6368.
[48] S. Krimm, J. Bandekar, Vibrational spectroscopy and conformation of peptides, polypeptides and proteins, in: C. Anfinson, J.T. Edsall, F.M. Richards (Eds.), Advances in Protein Chemistry, Academic Press, New York, 1986, pp. 181–365.
[49] J.C. Austin, T. Jordan, T.G. Spiro, Ultraviolet resonance Raman studies of proteins and related model compounds, in: R.J.H. Clark, R.E. Hester (Eds.), Biomolecular Spectroscopy, Part A, John Wiley & Sons Ltd., New York, 1993, pp. 55–127.
[50] Y. Wang, R. Purrello, S. Georgiou, T.G. Spiro, UVRR spectroscopy of the peptide bond. 2. Carbonyl H-bond effects on the ground- and excited-state structures of N-methylacetamide, J. Am. Chem. Soc. 113 (1991) 6368–6377.
[51] S.A. Oladepo, K. Xiong, Z. Hong, S.A. Asher, Elucidating peptide and protein structure and dynamics: UV resonance Raman spectroscopy, J. Phys. Chem. Lett. 2 (2011) 334–344.
[52] A.V. Mikhonin, S.V. Bykov, N.S. Myshakina, S.A. Asher, Peptide secondary structure folding reaction coordinate: correlation between UV Raman amide III frequency, psi Ramachandran angle, and hydrogen bonding, J. Phys. Chem. B 110 (2006) 1928–1943.
[53] Y. Deng, Z. Qian, Y. Luo, Y. Zhang, Y. Mu, G. Wei, Membrane binding and insertion of a pHLIP peptide studied by all-atom molecular dynamics simulations, Int. J. Mol. Sci. 14 (2013) 14532–14549.
[54] M. Eagleburger, J.W. Cooley, R. D. JiJi, Effects of fluidity on the ensemble structure of a membrane embedded α-helical peptide, unpublished results, (2013).